One-step transfer or exchange of arbitrary multipartite quantum states with a single-qubit coupler

Chui-Ping Yang,[1] Qi-Ping Su,[1] Shi-Biao Zheng,[2,*] and Siyuan Han[3,4,†]
[1]*Department of Physics, Hangzhou Normal University, Hangzhou, Zhejiang 310036, China*
[2]*Department of Physics, Fuzhou University, Fuzhou 350002, China*
[3]*Department of Physics and Astronomy, University of Kansas, Lawrence, Kansas 66045, USA*
[4]*Beijing National Laboratory for Condensed Matter Physics, Institute of Physics, Chinese Academy of Sciences, Beijing 100190, China*
(Received 4 June 2015; published 18 August 2015)

The transfer or exchange of multipartite quantum states is critical to the realization of large-scale quantum information processing and quantum communication. In this work, we demonstrate that by using a single quantum two-level system—*a qubit*—as a coupler, arbitrary multipartite quantum states (either entangled or separable) can be transferred or exchanged simultaneously between two sets of qubits. During the entire process, the coupler remains unexcited minimizing the effect of coupler decoherence on the process. This feature allows one to use qubits with rapid frequency tunability and a large range of frequency tuning, such as phase qubits, as couplers. Our findings offer the potential to significantly reduce the resources needed to construct and operate large-scale quantum information networks consisting of many multiqubit registers, memory cells, and processing units.

DOI: 10.1103/PhysRevB.92.054509 PACS number(s): 03.67.Lx, 85.25.Cp

I. INTRODUCTION

Entanglement arises from a nonclassical correlation between the constituents of multipartite quantum systems. It is one of the most profound and difficult to understand aspects of quantum physics. Entanglement is indispensable in quantum information science, as demonstrated by Shor's factorization algorithm [1] and various quantum key distribution protocols [2,3]. Recently, considerable interest has been devoted to the application of entangled states in quantum computation [4,5], quantum cryptography [2,6], teleportation [7–9], and quantum copying [10,11], and many previously unknown or unexpected properties of entanglement, such as entanglement swapping [10] and entanglement sudden death [12], have been discovered. Over the past decade, experimentalists have generated and verified entanglement in a variety of physical systems, including eight photons via linear optical devices [13,14], fourteen trapped ions [15], two atoms in cavity QED [16,17], two excitons in a single quantum dot [18], electron spins in two proximal nitrogen-vacancy centers [19], up to three superconducting qubits coupled via a single cavity [20–24], and five superconducting qubits coupled via capacitors [25].

Because transfer or exchange of arbitrary multipartite states (TEAMS) is of great importance to utilizing entanglement for quantum information processing (QIP) and quantum communication, it has attracted much attention. In principle, TEAMS can be accomplished by expanding either entanglement-based quantum teleportation protocols or nonteleportation protocols. For instance, many theoretical schemes [26–30] and experiments [31–35] have investigated how to transfer or exchange quantum states between two qubits using *entanglement-based* quantum teleportation protocols [7]. Among experiments, quantum state transfer between two superconducting qubits has been demonstrated in circuits consisting of multiple superconducting qubits coupled to planar resonators [36–39]. Alternatively, quantum state transfer or exchange can also be realized using nonteleportation protocols. For instance, by using photons (transmitted via an optical fiber) as the information carriers, the transfer of quantum states from one atom to another has been explored [40–42]. In addition, a quantum network, with single atoms placed in fiber-connected cavities, has been proposed, and the transfer of atomic quantum states and the creation of entanglement between two distant nodes of the network have been demonstrated experimentally [43].

Because in the work mentioned above the states being transferred or exchanged are single-particle states, it is not granted that these protocols can be applied to multipartite states without a substantial increase of resources (e.g., multiple EPR pairs). As quantum networks play an increasingly important role in scalable QIP, it is imperative to explore new and efficient methods to realizing TEAMS.

In this work, we consider a generic model system consisting of $2N$ qubits (e.g., spin-$\frac{1}{2}$ particles) coupled to a two-level coupler C (Fig. 1). The $2N$ qubits are divided arbitrarily into two sets, labeled as set A and set B, respectively, each containing N qubits. It is also assumed that qubits in the same set may or may not have direct intraset coupling, and that no *direct* coupling exists between qubits in different sets. The two-level coupler acts as an intermediary to allow quantum information, in the form of multipartite quantum states, to flow from A to B and vice versa. We show that for $N \geqslant 2$, by multiplexing a *single two-level coupler* it is sufficient to generate coupler-mediated effective interaction between the N pairs of qubits, and that arbitrary N-partite states can be transferred or exchanged between A and B in a *single* step. In addition, the coupler can also be used to mediate interactions between qubits in the same set, allowing the creation and manipulation of entanglement within each set.

We point out that the method proposed here has several distinctive advantages: (i) Only a two-level coupler is needed, and TEAMS can be performed simultaneously in a single step without the use of classical rf/microwave/optical pulses during the state transfer/exchange operation. This unique feature reduces the complexity of the circuits and operations. (ii) The two-level coupler C can be either a true quantum two-level system (TLS), such as an electron spin, or an effective TLS, such

*sbzheng11@163.com
†han@ku.edu

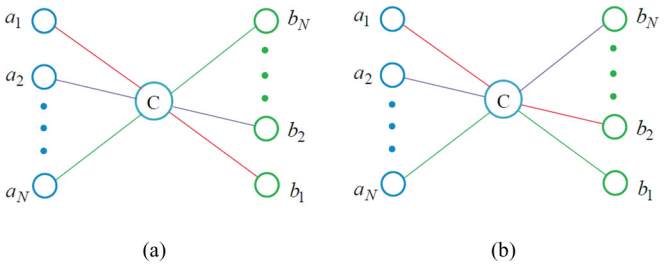

FIG. 1. (Color online) Two sets of qubits coupled by a two-level coupler C. Here, the large circle at the center represents the two-level coupler C, the smaller circles on the left (right) indicate the N qubits $a_1,a_2,\ldots,a_N$ ($b_1,b_2,\ldots,b_N$) in the register A (B) connected to the coupler C by lines with the same color, which form an interacting qubit pair. In (a), the N pairs of qubits are (a_1,b_1), (a_2,b_2), ..., and (a_N,b_N), while in (b) the N pairs of qubits are randomly chosen as, e.g., (a_1,b_2), (a_2,b_N), ..., and (a_N,b_1). For (a) and (b), arbitrary N-partite states can be transferred or exchanged between A and B. In addition, various entangled states of qubits in A and B can be generated by the same coupler-mediated qubit-qubit interaction.

as the two lowest levels of a superconducting qubit, so that the scheme can be applied to a large variety of physical quantum information networks. (iii) During the operation, the coupler stays mostly in its ground state so that the effects of quantum channel decoherence are greatly suppressed. This property allows the use of couplers with shorter decoherence time, but it has other desirable attributes such as rapid frequency tunability, design flexibility, or good scalability. (iv) It offers the flexibility of reconfiguring interactions between pairs of qubits, either intraset or interset, *in situ* to perform various QIP tasks without changing hardware wirings. (v) By connecting the qubits to multiple coupler qubits, the structure can be expanded readily into one- and two-dimensional quantum networks—a promising architecture for scalable QIP [44].

This paper is arranged as follows. In Sec. II, we derive the interaction Hamiltonian that governs the system dynamics of the $2N$ qubits plus one two-level coupler. It is evident from the Hamiltonian that N pairs of *in situ* programmable qubit-qubit superexchange interaction can occur in parallel without interference to each other, allowing the possibility of realizing TEAMS in a single step (e.g., by making all coupler-mediated effective pair interactions the same strength). In Sec. III, as an example, we describe in detail how to perform N-partite state exchange (swap) and transfer using this generic configuration. In Sec. IV, we propose a circuit QED-based implementation of the scheme. With realistic device and circuit parameters, numerical simulations show that the fidelity can reach 99.1% for Bell-state transfer and no less than 96.3% for Bell-state swap. In Sec. V, we summarize the key result and its impact on the future development of quantum information science.

II. HAMILTONIAN

Without the loss of generality, we consider two sets of otherwise noninteracting qubits connected to a two-level coupler C, hereafter referred to as coupler C for simplicity, as illustrated in Fig. 1(a). The first set contains N qubits $\{a_1,a_2,\ldots,a_j,\ldots,a_N\}$ while the second set contains the remaining N qubits $\{b_1,b_2,\ldots,b_k,\ldots,b_N\}$. The two logic states of qubit a_j (b_k) are labeled as $|0\rangle_{a_j(b_k)}$ and $|1\rangle_{a_j(b_k)}$, and that of the coupler C are denoted as $|g\rangle_c$ and $|e\rangle_c$, respectively. As will be shown, either a bosonic mode or an atom can act as qubit a_j (b_k), and we will focus our discussions on bosonic qubits. In this case, the state flipping operators for qubit a_j correspond to the bosonic annihilation and creation operators $\hat{a}_j$ and $\hat{a}_j^+$, which satisfy $\hat{a}_j|0\rangle_{a_j}=0$, $\hat{a}_j|1\rangle_{a_j}=|0\rangle_{a_j}$, and $\hat{a}_j^+|0\rangle_{a_j}=|1\rangle_{a_j}$. Analogously, the bosonic operators $\hat{b}_k$ and $\hat{b}_k^+$ are equivalent to the state flipping operators for qubit b_k. We define the raising and lowering operators $\sigma=|g\rangle_c\langle e|$ and $\sigma^+=|e\rangle_c\langle g|$ for the coupler C. The discussion below is based on Fig. 1(a). However, it should be mentioned that the results can directly apply to Fig. 1(b) to accomplish the same tasks, by mapping the large detuning conditions, required for the qubit pairs (a_1,b_1), (a_2,b_2), ..., and (a_N,b_N), to the qubit pairs (a_1,b_2), (a_2,b_N), ..., and (a_N,b_1) in Fig. 1(b), respectively.

In general, qubits a_j and b_k can be tuned to have the same detuning with respect to the coupler's transition frequency ω_c. However, for the sake of simplicity, we set $j=k$ in the following discussion. Suppose qubit a_j (b_j) is coupled to the coupler C, with coupling strength g_j (μ_j) and detuning Δ_j. In the interaction picture, the Hamiltonian of the whole system is given by

$$H_I=\sum_{j=1}^{N}(g_j e^{i\Delta_j t}\hat{a}_j\sigma^+ + \mu_j e^{i\Delta_j t}\hat{b}_j\sigma^+ + \text{H.c.}), \quad (1)$$

where $\Delta_j=\omega_c-\omega_{aj}=\omega_c-\omega_{bj}$ (Fig. 2), and ω_{aj} (ω_{bj}) is the frequency of qubit a_j (b_j).

Under the large detuning condition $\Delta_j \gg g_j,\mu_j$, the two sets of qubits do not exchange energy with the coupler. However, the coupler can mediate N independent pairwise superexchange interactions between the two sets of $2N$ qubits. Qubit a_j is only coupled to qubit b_j when the detunings satisfy the following conditions:

$$\frac{|\Delta_j-\Delta_k|}{\Delta_j^{-1}+\Delta_k^{-1}} \gg g_j g_k,\ g_j\mu_k,\ \mu_j\mu_k;\ j\neq k. \quad (2)$$

Then we obtain the effective Hamiltonian $H_{\text{eff}}=H_0+H_{\text{int}}$, with

$$H_0=\sum_{j=1}^{N}\left(\frac{g_j^2}{\Delta_j}\hat{a}_j\hat{a}_j^\dagger+\frac{\mu_j^2}{\Delta_j}\hat{b}_j\hat{b}_j^\dagger\right)|e\rangle\langle e| - \sum_{j=1}^{N}\left(\frac{g_j^2}{\Delta_j}\hat{a}_j^\dagger\hat{a}_j+\frac{\mu_j^2}{\Delta_j}\hat{b}_j^\dagger\hat{b}_j\right)|g\rangle\langle g|, \quad (3)$$

$$H_{\text{int}}=\sum_{j=1}^{N}\lambda_j(\hat{a}_j\hat{b}_j^\dagger+\hat{a}_j^\dagger\hat{b}_j)(|e\rangle\langle e|-|g\rangle\langle g|), \quad (4)$$

where $\lambda_j=g_j\mu_j/\Delta_j$. The first (second) term in the first bracket of H_0 is an ac Stark shift of the level $|e\rangle$ of the coupler C, induced by the interaction with qubit a_j (b_j), while the first (second) term in the second bracket of H_0 is an ac Stark shift of the level $|g\rangle$ of the two-level coupler, induced by the interaction with qubit a_j (b_j). Here and below, we have defined $|g\rangle\equiv|g\rangle_c$ and $|e\rangle\equiv|e\rangle_c$ for simplicity.

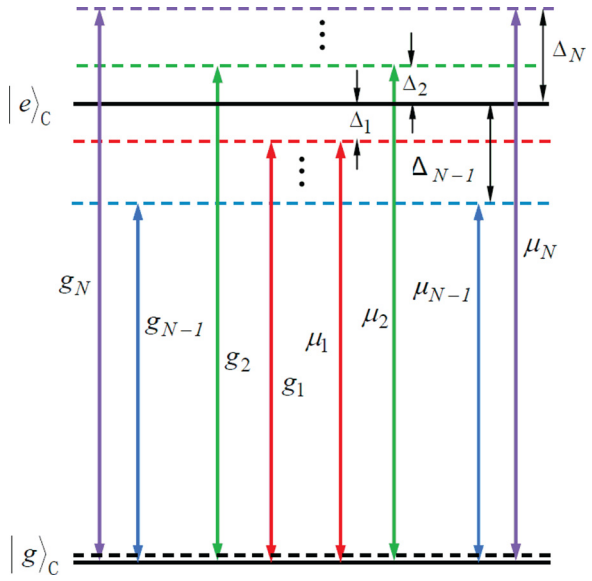

FIG. 2. (Color online) Illustration of qubit-coupler dispersive interaction. The two horizontal solid lines represent the two energy levels of the coupler C. The bottom dashed line represents the common ground energy level of the $2N$ qubits, while the top dashed lines in different colors represent the higher-energy levels of the $2N$ qubits, respectively. A vertical line, linked to the bottom dashed line and a top dashed line, represents the level spacing between the two energy levels of a qubit. The frequency of qubit a_j (b_j) is labeled as ω_{aj} (ω_{bj}) (not shown), while the frequency of the coupler C is denoted as ω_c (not shown). Qubit a_j (b_j) is dispersively coupled to the coupler C with coupling constant g_j (μ_j) and detuning Δ_j ($j = 1,2,\ldots,N$). Here, $\Delta_j = \omega_c - \omega_{aj} = \omega_c - \omega_{bj}$.

To simplify discussions, hereafter we set $g_j = \mu_j$ and $\omega_{aj} = \omega_{bj} = \omega_j$, which can be realized readily by design and fabrication. Consequently, the qubits a_j and b_j have the same detuning Δ_j. It is also understood that $\omega_i \neq \omega_j$ and $g_i \neq g_j$ for $i \neq j$. In this way, each pair of qubits has its own unique frequency and qubit-coupler interaction strength, while all pairs have the same effective coupler-mediated interaction strength. In a new interaction picture with respect to the Hamiltonian H_0, we have $H'_{\rm int} = e^{iH_0t}H_{\rm int}e^{-iH_0t} = H_{\rm int}$. When the coupler C is initially in the ground state $|g\rangle$, it will remain in this state throughout the interaction as the Hamiltonian $H_{\rm int}$ cannot induce any transition for the coupler. In this case, based on Eq. (4) and $H'_{\rm int} = H_{\rm int}$, the Hamiltonian $H'_{\rm int}$ is reduced to

$$H_e = -\sum_{j=1}^{N}\lambda_j(\hat{a}_j\hat{b}_j^\dagger + \hat{a}_j^\dagger\hat{b}_j), \tag{5}$$

which is the effective Hamiltonian governing the dynamics of the two sets of qubits.

The two sets of qubits can be any type of qubits, such as bosonic qubits or atomic qubits (e.g., artificial atoms or natural atoms). In principle, we can employ this effective Hamiltonian to implement several fundamental quantum operations on two sets of qubits, such as entanglement swap, multiqubit logic gates, and creation of quantum entanglement in or between two sets of qubits. As a concrete example, in the next section we explicitly show how to apply this Hamiltonian to implement TEAMS between two sets of bosonic qubits.

As a final note, we point out that the condition $g_j = \mu_j$ is unnecessary. As shown in Appendix A, for the case of $g_j \neq \mu_j$, the effective Hamiltonian (5) can be obtained by setting the detuning of the qubit a_j slightly different from that of qubit b_j ($j = 1,2,\ldots,N$).

III. QUANTUM STATE SWAPPING AND TRANSFER

Let us go back to Fig. 1(a), where any initially unentangled state of the first set of N bosonic qubits $(a_1,a_2,\ldots,a_N)$ and the second set of N bosonic qubits $(b_1,b_2,\ldots,b_N)$ can be described by the joint state $|\psi_{\rm A}(0)\rangle \otimes |\psi_{\rm B}(0)\rangle$. Here, the first (second) part of the product is the initial state of the first (second) set of N qubits, taking a general form of $|\psi_{\rm A}(0)\rangle = \sum_{n_j=0}^{1} c_{\{n_j\}}\prod_{j=1}^{N}|n_j\rangle_{a_j}$ ($|\psi_{\rm B}(0)\rangle = \sum_{m_k=0}^{1} d_{\{m_k\}}\prod_{k=1}^{N}|m_k\rangle_{b_k}$). The subscript a_j (b_k) represents qubit a_j (b_k), $c_{\{n_j\}}$ is the coefficient of the component $\prod_{j=1}^{N}|n_j\rangle_{a_j}$ of the initial state for the qubits $(a_1,a_2,\ldots,a_N)$, and the same notation applies to $d_{\{m_k\}}$ for the qubits $(b_1,b_2,\ldots,b_N)$. In terms of $|1_j\rangle_{a_j} = \hat{a}_j^\dagger|0\rangle_{a_j}$ and $|1_k\rangle_{b_k} = \hat{b}_k^\dagger|0\rangle_{b_k}$, we can write down the initial state as

$$|\psi_{\rm A}(0)\rangle \otimes |\psi_{\rm B}(0)\rangle = \sum_{n_j=0,1} c_{\{n_j\}}\sum_{m_k=0,1} d_{\{m_k\}}\prod_{j=1}^{N}\prod_{k=1}^{N}\left(\hat{a}_j^{+n_j}\hat{b}_k^{+m_k}|0\rangle_a|0\rangle_b\right), \tag{6}$$

where $|0\rangle_a = |0\rangle_{a_1}\cdots|0\rangle_{a_N}$, $|0\rangle_b = |0\rangle_{b_1}\cdots|0\rangle_{b_N}$, $(\hat{a}_j^+)^0 = 1$, and $(\hat{b}_k^+)^0 = 1$.

For bosonic qubits, the operators $(\hat{a}_j,\hat{a}_j^+)$ and $(\hat{b}_j,\hat{b}_j^+)$ obey $[\hat{a}_j,\hat{a}_j^+] = [\hat{b}_j,\hat{b}_j^+] = 1$. The effective Hamiltonian H_e leads to the transformations $e^{-iH_et}\hat{a}_j^\dagger e^{iH_et} = \cos(\lambda_j t)\hat{a}_j^\dagger + i\sin(\lambda_j t)\hat{b}_j^\dagger$, and $e^{-iH_et}\hat{b}_j^\dagger e^{iH_et} = \cos(\lambda_j t)\hat{b}_j^\dagger + i\sin(\lambda_j t)\hat{a}_j^\dagger$. These transformations have the following property: (i) By setting $|\lambda_j| = \lambda$, then $g_j\mu_j/|\Delta_j| = \lambda$ (independent of j). This condition can be met by using frequency-tunable qubits (or resonators). In the case of fixed frequency resonators, one can design and fabricate the qubits a_j and b_j to have the proper frequencies ($\omega_{aj} = \omega_{bj} = \omega_j$) and coupling strengths (g_j, μ_j), respectively, and to set $|\Delta_j| = g_j\mu_j/\lambda$ accordingly. (ii) For $\lambda t = \pi/2$, we obtain $e^{-iH_et}\hat{a}_j^\dagger e^{iH_et} = i^{\lambda_j/\lambda}\hat{b}_j^\dagger$ and $e^{-iH_et}\hat{b}_j^\dagger e^{iH_et} = i^{\lambda_j/\lambda}\hat{a}_j^\dagger$. Accordingly, we have $e^{-iH_et}\hat{a}_j e^{iH_et} = -i^{\lambda_j/\lambda}\hat{b}_j$ and $e^{-iH_et}\hat{b}_j e^{iH_et} = -i^{\lambda_j/\lambda}\hat{a}_j$. These unitary transformations will be employed in the derivation of Eq. (7) below.

Under the Hamiltonian H_e, the state of the subsystem, consisting of the $2N$ qubits in sets A and B, after an evolution time $t = \pi/(2\lambda)$ is given by

$$|\psi_{\rm AB}(t)\rangle = e^{-iH_et}\,|\psi_{\rm A}(0)\rangle \otimes |\psi_{\rm B}(0)\rangle = \sum_{n_j=0,1} c_{\{n_j\}}\sum_{m_k=0,1} d_{\{m_k\}}\prod_{j=1}^{N}\prod_{k=1}^{N} \times[(i)^{n_j\lambda_j/\lambda}(i)^{m_k\lambda_k/\lambda}(\hat{b}_j^\dagger)^{n_j}(\hat{a}_k^\dagger)^{m_k}|0\rangle_a|0\rangle_b]$$

$$= \sum_{m_k=0,1} d_{\{m_k\}} \prod_{k=1}^{N} (i)^{m_k \lambda_k/\lambda} |m_k\rangle_{a_k}$$

$$\otimes \sum_{n_j=0,1} c_{\{n_j\}} \prod_{j=1}^{N} (i)^{n_j \lambda_j/\lambda} |n_j\rangle_{b_j}, \quad (7)$$

where $\lambda_j/\lambda = \pm 1$ and $\lambda_k/\lambda = \pm 1$. Note that in the last two lines of Eq. (7), the first part of the product represents the N-qubit state of $(a_1, a_2, \ldots, a_N)$ while the second part is that of $(b_1, b_2, \ldots, b_N)$.

After returning to the original interaction picture, the state of the whole system, $|\psi'_{\rm ABC}(t)\rangle = e^{-iH_0 t}|\psi_{\rm AB}(t)\rangle|\psi_{\rm c}(t)\rangle$, can be further written as $|\psi'_{\rm ABC}(t)\rangle = |\psi'_{\rm AB}(t)\rangle \otimes |g\rangle_{\rm c}$. By letting H_0 act on the state $|\psi_{\rm AB}(t)\rangle$, we obtain a decomposition of $|\psi'_{\rm AB}(t)\rangle = |\psi_{\rm A}(t)\rangle \otimes |\psi_{\rm B}(t)\rangle$ with

$$|\psi_{\rm A}(t)\rangle = \sum_{m_k=0,1} d_{\{m_k\}} \prod_{k=1}^{N} (e^{i\phi_k m_k \pi}|m_k\rangle_{a_k}), \quad (8)$$

$$|\psi_{\rm B}(t)\rangle = \sum_{n_j=0,1} c_{\{n_j\}} \prod_{j=1}^{N} (e^{i\theta_j n_j \pi}|n_j\rangle_{b_j}), \quad (9)$$

where $\phi_k = (\lambda_k + g_k^2/\Delta_k)/(2\lambda)$ and $\theta_j = (\lambda_j + \mu_j^2/\Delta_j)/(2\lambda)$. This is equivalent to the quantum state swap operation plus single-qubit phase shifts $e^{i\phi_k\pi}$ ($e^{i\beta_j\pi}$) on the state $|1\rangle$ of qubit a_k (b_j). These additional phase shifts can be corrected by local single-qubit rotations $e^{-i\phi_k\pi\hat{a}_k^\dagger\hat{a}_k}$ and $e^{-i\theta_j\pi\hat{b}_j^\dagger\hat{b}_j}$. Notice that the multiplexed quantum state exchange protocol described above becomes the state transfer protocol by initializing all qubits in the second (i.e., receiving) set in the state $|0\rangle$. More importantly, because the states $|\psi_{\rm A}(0)\rangle$ and $|\psi_{\rm B}(0)\rangle$ considered above take a general form, the protocol can be applied directly to swap or transfer any type of multipartite entanglement, such as the GHZ state $|00\cdots0\rangle + |11\cdots1\rangle$, the W state $\frac{1}{\sqrt{N}}(|00\cdots001\rangle + |00\cdots010\rangle + \cdots + |10\cdots000\rangle)$, the cluster state, and so on, between the two sets of multiple qubits.

It should be mentioned that in reality, a physical coupler usually has more than two levels. However, if the coupler is a nonlinear quantum element such as a superconducting qubit, population leakage out of the two-dimensional Hilbert space formed by $|g\rangle$ and $|e\rangle$ of the coupler can be made negligible by choosing proper coupler parameters. In contrast, when the coupler is a single-mode resonator [45], the probability of population leaking into higher energy levels of the coupler could be significantly greater due to its uniform energy level spacing. This problem becomes apparent as the number of qubits increases.

The quantum dynamics of two bosonic qubits/resonators coupled by a superconducting qubit as a quantum switch has been studied previously in [46,47]. However, although our method of TEAMS is based on the same type of coupler-mediated dispersive interaction between qubits described in [46,47], it is not a simple extension of the latter. The reasons for this are as follows. First, the physical mechanism of our scheme is quite different from that of the quantum switch proposal [46,47]. For the latter, the intercavity cross coupling between the two resonators is an indispensable resource for quantum state transfer or exchange, which can be made negligibly small according to the recent experiments [37,48–50] and is not required in our scheme. Second, the methods in [46,47] would require the use of N couplers for N pairs of qubits/resonators. One of the advantages of our method is that by utilizing the "frequency multiplexing" capability of our effective Hamiltonian, each qubit in one set is coupled uniquely to only one of the qubits in the other set, and all N pairwise interactions occur concurrently, so that one-step TEAMS between the two N-qubit sets with only one coupler qubit, rather than N couplers, becomes possible.

It is noted that if one chooses to perform TEAMS between two sets of resonators, the preparation of the initial state of the resonators would in general require the use of additional qubits as well as tunable qubit-resonator couplings [51–54]. For example, this task could be accomplished by coupling one ancilla qubit to each resonator [48,55]. However, because the main objective of this work is to show how to perform TEAMS in a single step, we assume that the states to be transferred or exchanged already exist. Thus, we will not discuss the details of how to prepare the initial states of the resonators.

The two-level coupler is assumed to be a frequency-tunable (by several hundred MHz within a few ns) superconducting qubit (also known as an artificial atom) [25,56–59]. Generally speaking, it is highly desirable to use qubits with frequency and coupling strength (g_j and μ_j) both tunable to implement the proposed one-step TEAMS, as the double tunability would provide maximum operational and configurational flexibility in satisfying all required conditions, in particular $|\lambda_j| = g_j\mu_j/|\Delta_j| = \lambda$. In practice, however, frequency tunability is readily available for artificial atoms and to a less extent for resonators [60,61], while tunable coupling strength is significantly more difficult to obtain.

We emphasize that an assumption of uniform effective coupling strength is unnecessary, and it is only used to clarify the discussion above. For instance, a manufactured circuit with fixed coupling strengths may have j-dependent effective coupling strengths λ_j. In this case, TEAMS cannot be completed by turning on/off the effective coupling for all pairs of qubits simultaneously. Fortunately, this problem can be circumvented by relaxing the strong condition to a weaker one: instead of requiring all λ_j's to have the same magnitude, they can be different as long as the condition $\omega_{aj} = \omega_{bj} = \omega_j \neq \omega_i$ ($j \neq i$) is still satisfied. The weaker condition can be met by using frequency-tunable qubits or resonators. A simple case to consider is when the effective qubit-coupler coupling strengths for all $2N$ qubits (resonators) are nonidentical or approximately equal. Experimentally, this is the easiest to realize and most likely to be encountered. With this setup, all one needs to do is to switch on the effective dispersive interaction between qubits a_j and b_j at a proper time $\tau_j = t_{\max} - t_j$ by tuning their frequencies to have the proper Δ_j, where $t_{\max} = \max(\pi/2\lambda_1, \pi/2\lambda_2, \ldots, \pi/2\lambda_N)$ and $t_j = \pi/2\lambda_j$, and to switch off all the effective interactions at the time $t_{\max}$ by tuning the coupler frequency ω_c far off-resonance with those of all $2N$ qubits. In the last step, the coupler is used essentially as an N-channel switch [46,47] to simultaneously cut off the effective interaction between all pairs of qubits.

TABLE I. Parameters for a system of four resonators coupled by a Xmon qubit. The values of ω_{a_j}, ω_{b_j}, Q_{a_j}, and Q_{b_j} ($j = 1,2$) are estimated for $\alpha = 8.1$ (both Bell-state transfer and exchange), $\omega_c/2\pi = 6.0$ GHz, and $g/2\pi = 40$ MHz. Here, $Q_{a_j} = \omega_{a_j}\kappa_{a_j}^{-1}$ and $Q_{b_j} = \omega_{b_j}\kappa_{b_j}^{-1}$. Notice that T_1 and T_2 can be made to be on the order of 20–60 μs for state-of-the-art superconducting qubits [49,77–80]. Superconducting CPW (coplanar waveguide) resonators with a quality factor $Q \sim 10^6$ have been experimentally demonstrated [61–63]. In addition, the coupling strength $g/2\pi \sim 360$ MHz has been reported for a superconducting qubit coupled to a one-dimensional standing-wave CPW resonator [81].

	Symbol	Bell-state transfer	Bell-state exchange
Resonator photon lifetime	$\kappa_{a_1}^{-1},\kappa_{b_1}^{-1},\kappa_{a_2}^{-1},\kappa_{b_2}^{-1}$	5 μs	5μs
Coupler energy relaxation time	$T_1 = \gamma^{-1}$	15 μs	15 μs
Coupler dephasing time	$T_2 = \gamma_\varphi^{-1}$	10 μs	10 μs
Coupling strength	g	$2\pi \times 40$ MHz	$2\pi \times 40$ MHz
Coupler frequency at working point	$\omega_c/2\pi$	6.0 GHz	6.0 GHz
Resonator frequency, pair I	$\omega_{a_1}/2\pi,\omega_{b_1}/2\pi$	5.676 GHz	5.676 GHz
Resonator frequency, pair II	$\omega_{a_2}/2\pi,\omega_{b_2}/2\pi$	6.324 GHz	6.324 GHz
Resonator quality factor, pair I	Q_{a_1}, Q_{b_1}	1.78×10^5	1.78×10^5
Resonator quality factor, pair II	Q_{a_2}, Q_{b_2}	1.98×10^5	1.98×10^5

The coupling between the resonators and the coupler qubit can be effectively turned on (off) by adjusting the level spacings of the coupler qubit [48,50]. When the coupler qubit frequency is highly detuned from the resonator frequencies, the couplings are effectively switched off, and when the coupler qubit frequency is detuned from the resonator frequencies by a suitable amount they are dispersively coupled, as in the case discussed above. For a superconducting coupler qubit, the level spacings can be readily adjusted by varying external control parameters (e.g., magnetic flux applied to phase, transmon, Xmon, or flux qubits; see, e.g., [25,56–59]).

It should be pointed out that for fixed-frequency qubits and resonators, using a common capacitor as a coupler could not accomplish the task because the capacitor-mediated interaction between qubits that have the same frequency cannot be turned off. For the sake of concreteness, let us consider the case of four ($2N = 4$) fixed-frequency resonators with parameters listed in Table I, connected to a common coupler with the same coupling constant g. It is obvious that in this case transferring or exchanging quantum states (e.g., Bell states) between two pairs of resonators could not be accomplished if the coupler was a capacitor. In stark contrast, when using a qubit as the coupler, the coupler-mediated dispersive interaction between all qubit pairs can be easily switched on (off) by tuning the frequency of the coupler qubit to 6 GHz ($|\omega_c - \omega_{i=1,2}| > 1$ GHz $\gg g$).

IV. EXPERIMENTAL IMPLEMENTATION

In practice, the proposed scheme can be implemented using either the artificial atoms (e.g., superconducting qubits) or resonators [e.g., superconducting coplanar waveguide (CPW) resonators] as the physical objects to demonstrate the proposed one-step TEAMS protocol. The artificial atoms have the advantage of tunable frequency, better separation between the computational states and the noncomputational ones because they are nonlinear oscillators, and ease of initial-state preparation. On the other hand, a high-Q CPW resonator is comparatively easier to design and fabricate. For example, CPW resonators with a quality factor on the order of 10^6 (i.e., about 30 μs of the lifetime of photons for a 6 GHz resonator) have been demonstrated with a single layer of sputtered superconducting films [62–64]. In addition, frequency-tunable resonators have also been demonstrated recently [60,61].

In the example discussed below, we choose resonators as the realization of bosonic qubits for the following reasons: (i) Systems of superconducting resonators and qubits have been considered one of the most promising candidates for quantum information processing [65–68], and there is a growing interest in quantum information processing based on microwave photon qubits. Within circuit QED, several theoretical proposals have been put forward for utilizing microwave photons stored in two superconducting CPW resonators as qubits/qudits for quantum gates [69–72]. (ii) Microwave photons have been considered as candidates for quantum memories [61,73–75]. When performing quantum information processing, TEAMS between different multiqubit memory banks would become a ubiquitous task. (iii) Because it is generally more difficult to tune the frequency of the resonators than artificial atoms, and because linear resonators are a poor realization of qubits, if our scheme can be demonstrated to work well with fixed frequency and coupling strength resonators, it would work better and/or be easier to implement with frequency-tunable artificial atoms or resonators. In other words, we choose a more difficult case to study.

Let us now consider four fixed-frequency superconducting coplanar waveguide (CPW) resonators, capacitively coupled to a superconducting Xmon coupler [76] as illustrated in Fig. 3. We emphasize again that using frequency-tunable resonators [60,61] or artificial atoms would make the implementation considerably easier. For simplicity, we use (a_1,a_2,b_1,b_2) to denote the four resonators. For the setup here, a_j (b_j) is a bosonic mode of the resonator a_j (b_j), and the two logic states of the qubit a_j (b_j) are represented by the vacuum state and the single-photon state of the bosonic mode of resonators a_j (b_j) ($j = 1,2$). In the following, we first present a general discussion on the fidelity of the operation. To quantify the operational fidelity of the proposed protocol, we numerically calculate the fidelity for transferring and exchanging each of the four Bell states $|\psi^\pm\rangle = \frac{1}{\sqrt{2}}(|01\rangle \pm |10\rangle)$ and $|\phi^\pm\rangle = \frac{1}{\sqrt{2}}(|00\rangle \pm |11\rangle)$ between the two pairs of qubits (i.e., the case of $N = 2$).

In the above discussions, we have considered each qubit as a two-level bosonic mode and defined the operators $\hat{a}_j$, $\hat{b}_j$,

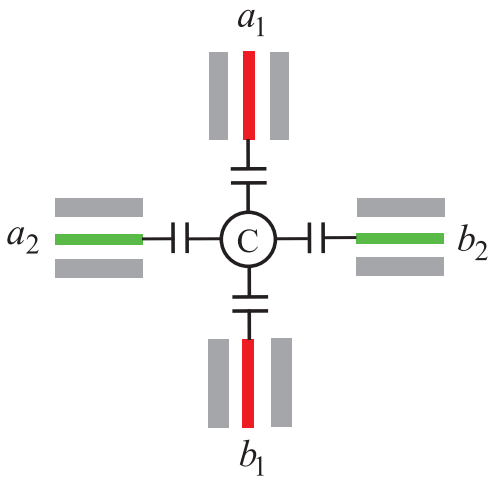

FIG. 3. (Color online) Setup for four resonators a_1,a_2,b_1,b_2 coupled by a superconducting Xmon coupler (i.e., the circle C). Each resonator here is a one-dimensional coplanar waveguide resonator. The superconducting Xmon qubit is capacitively coupled to each resonator via a capacitance.

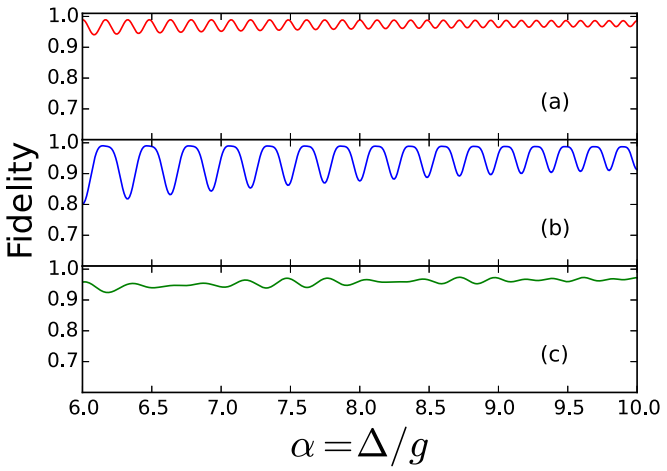

FIG. 4. (Color online) Fidelity vs α for the Bell-state transfer. Part (a) corresponds to transferring the Bell state $|\psi^+\rangle$. Part (b) corresponds to transferring the Bell state $|\psi^-\rangle$. Part (c) is for transferring the other two Bell states $|\phi^\pm\rangle$. Numerical simulation shows that the fidelity for transferring both Bell states $|\phi^\pm\rangle$ is the same.

$\hat{a}_j^+$, and $\hat{b}_j^+$ using the two energy eigenstates $|0\rangle$ and $|1\rangle$ as the computational basis states. It is noted that during the operation, more than a single photon could reside in each resonator when the large detuning conditions (2) are not well satisfied. For this reason, we treat the above-defined operators $\hat{a}_j$, $\hat{b}_j$, $\hat{a}_j^+$, and $\hat{b}_j^+$ as the usual photon annihilation and creation operators introduced in quantum optics. Note that after this replacement, the Hamiltonian H_I in the interaction picture, describing the interaction of the four resonators with the Xmon coupler, takes the same form as that given in Eq. (1) with $N = 2$. By doing this, the effects of excited states of the resonators are taken into account.

When the dissipation and dephasing are included, the dynamics of the open system is determined by the following master equation:

$$\frac{d\rho}{dt} = -i[H_I,\rho] + \sum_{j=1}^{2}\kappa_{a_j}\mathcal{L}[\hat{a}_j] + \sum_{j=1}^{2}\kappa_{b_j}\mathcal{L}[\hat{b}_j] + \gamma\mathcal{L}[\sigma] + \gamma_\varphi(\sigma_z\rho\sigma_z - \rho), \quad (10)$$

where H_I is the interaction Hamiltonian given in Eq. (1), $\sigma_z = |e\rangle\langle e| - |g\rangle\langle g|$, and $\mathcal{L}[\Lambda] = \Lambda\rho\Lambda^+ - \Lambda^+\Lambda\rho/2 - \rho\Lambda^+\Lambda/2$ (with $\Lambda = \hat{a}_j,\hat{b}_j,\sigma$). In addition, κ_{a_j} (κ_{b_j}) is the decay rate of the resonator mode a_j (b_j), γ is the energy relaxation rate for the level $|e\rangle$, and γ_φ is the dephasing rate of the level $|e\rangle$ of the coupler.

The numerical simulation is carried out by solving the master equation (10), which describes the dynamics of four resonators coupled to a superconducting Xmon. As shown in Table I [49,62–64,76–80], the simulation takes the effects of dissipation and dephasing on the fidelity into account. Specifically, we selected a conservative set of resonator and Xmon parameters in the numerical simulation to demonstrate experimental feasibility. In addition, assuming all coupling constants are equal, $g_1 = \mu_1 = g_2 = \mu_2 \equiv g = 2\pi \times 40$ MHz (again this is an undesirable situation). The fidelity of the operations is given by $\mathcal{F} = \sqrt{\langle\psi_{\rm id}|\widetilde{\rho}|\psi_{\rm id}\rangle}$ [81], where $|\psi_{\rm id}\rangle = |\psi_{\rm A}(t)\rangle|\psi_{\rm B}(t)\rangle|g\rangle_{\rm c}$, with $|\psi_{\rm A}(t)\rangle$ given in Eq. (8) and $|\psi_{\rm B}(t)\rangle$ in Eq. (9), is the output state for an ideal system (i.e., without dissipation, dephasing, and leakage to high excited states) after completing the operations, and $\widetilde{\rho}$ is the final density operator of the system.

In the numerical simulation, we set $\Delta \equiv \Delta_1 = -\Delta_2$. The simulated fidelity as a function of the dimensionless detuning $\alpha \equiv \Delta/g$ in the range of $6 \leqslant \alpha \leqslant 10$ for Bell-state transfer and exchange is shown in Figs. 4 and 5, respectively. For $\alpha \equiv \Delta/g \sim 8.1$, the fidelity of transferring the four Bell states

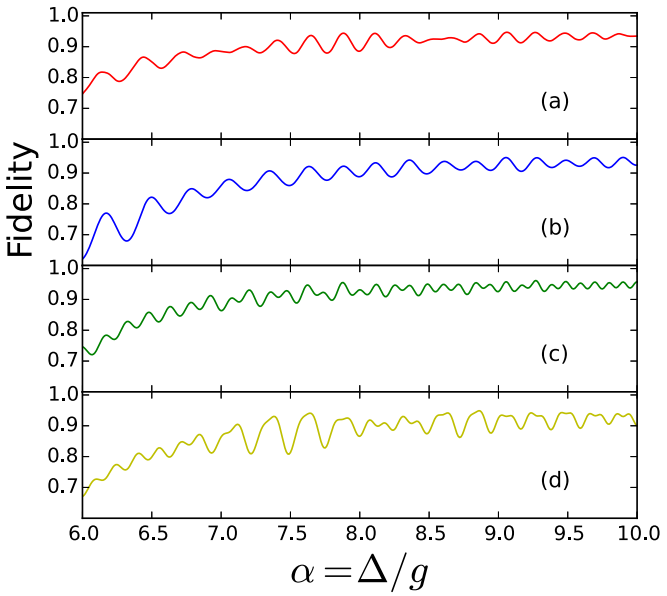

FIG. 5. (Color online) Fidelity vs α for the Bell-state exchange. Part (a) corresponds to exchanging $|\psi^+\rangle$ with $|\psi^-\rangle$. Part (b) corresponds to exchanging $|\phi^+\rangle$ with $|\phi^-\rangle$. Part (c) corresponds to exchanging $|\phi^\pm\rangle$ with $|\psi^+\rangle$. Part (d) is for exchanging $|\phi^\pm\rangle$ with $|\psi^-\rangle$.

$|\psi^{\pm}\rangle$ and $|\phi^{\pm}\rangle$ from the resonators (a_1,a_2) to (b_1,b_2) or vice versa is equal to or better than 96.2%, while for exchanging $|\psi^{+}\rangle$ with $|\psi^{-}\rangle$, $|\phi^{+}\rangle$ with $|\phi^{-}\rangle$, $|\phi^{\pm}\rangle$ with $|\psi^{+}\rangle$, and $|\phi^{\pm}\rangle$ with $|\psi^{-}\rangle$, the fidelity is 94.3%, 93.3%, 94.9%, and 91.8%, respectively. Furthermore, the high fidelity is hardly affected by weak residual inter-resonator cross-talk, as is often the case in experimental situations (see Appendix B). However, it should be pointed out that the value of the detuning parameter α at which the high fidelity is achieved depends on other parameters, such as the photon decay rate of the resonators, and thus it is not universal. In experiments, α needs to be fine-tuned to obtain a high fidelity. Finally, note that the operational time depends on the value of α. For the optimal point $\alpha\sim 8.1$, the operational time for the Bell state transfer or exchange is estimated to be ~ 0.05 μs, which is much shorter than the decoherence times of the resonators and the coupler used in our numerical simulation.

As discussed previously, one of the advantages of the single-step TEAMS method proposed here is that the coupler remains separable from the qubits, and it stays mostly in the ground state so that the effects of the coupler's decoherence on the fidelity of TEAMS is significantly reduced. Numerical simulations were performed to confirm this property, and the result confirms that for Bell-state transfer (exchange), the population of the coupler's excited state $|e\rangle$ (averaged over the entire operation time) is $0.014 \leqslant \overline{P}_e \leqslant 0.040$ $(0.008 \leqslant \overline{P}_e \leqslant 0.012)$ for the operations described above.

As the above example and parameters listed in Table I show, our scheme does not require the use of tunable resonator-coupler coupling strength and/or tunable frequency resonators. Furthermore, $g_j = \mu_j$ is not a necessary condition, and it is chosen only to simplify discussions. The strong condition that needs to be satisfied for simultaneous TEAMS is that the effective pairwise coupling strength $\lambda_j = g_j\mu_j/\Delta_j$ should have the same value for all $j = 1,2,\ldots,N$ qubit pairs. Therefore, although it would be more convenient, our scheme does not require tunable resonator-qubit coupling strength g_j and μ_j. For example, it is straightforward to design and to fabricate pairs of resonators a_j and b_j to have j-dependent frequency ω_j and coupling strength g_j such that $|\lambda_j| = g_j^2/|\Delta_j| = \lambda$. When the resonator frequencies can be individually tuned, the scheme also works for nonidentical effective coupling strengths. In this case, the TEAMS can be completed by switching on the effective dispersive interaction of each pair at a different time commensurate with its effective coupling strength and switching off the coupler-mediated effective interactions of all pairs at the same time.

It is worthwhile to discuss the advantage of utilizing positive as well as negative detunings. Because our scheme essentially explores the frequency multiplexing property of the effective Hamiltonian (5), it will encounter the "frequency crowding" problem. Because the system dynamics does not depend on the signs of detunings according to Eqs. (6)–(9), utilizing the positive as well as the negative detunings would double the maximum number of qubits that can be accommodated by a given circuit. This advantage is most clearly demonstrated by the example presented above: when all four resonators have the same coupling strength to the coupler, the only way to satisfy $\lambda_1 = |\lambda_2| = \lambda$ is to have $\Delta_1 = -\Delta_2$.

We would like to point out that although the proposed scheme of TEAMS can be implemented for a small number of qubits or resonators with fixed frequency and/or coupling strength, it is in general desirable and even necessary to have the frequency tunability for a moderate number of qubits or resonators. This is especially true if one wants to realize the reconfigurable network illustrated in Fig. 1. Note that tunable frequency artificial atoms are readily available, and tunable superconducting resonators have been demonstrated by incorporating nonlinear elements, such as a small dc SQUID, into the design [60,61].

V. CONCLUSION

We have shown that simultaneously transferring or swapping arbitrary multipartite quantum states between two sets of otherwise noninteracting qubits each having a 2^N-dimensional Hilbert space can be achieved using a single two-level coupler. This result means that arbitrary N-qubit states that span a 2^N-dimensional Hilbert space can be transferred or exchanged between two N-qubit registers in a single step via a coupler whose Hilbert space is two-dimensional only. In addition, during the entire process the coupler remains separable from the qubits and stays mostly in the ground state throughout the entire process, thus suppressing the undesirable effects of coupler decoherence. The method presented here for simultaneously transferring or swapping arbitrary N-partite states in a single step is of great interest and fundamental importance in quantum information science. If realized experimentally, it would be a big step forward in the direction of building scalable quantum information processing networks because in principle the operation time required is independent of the number of qubits involved. In addition, as a concrete example we show that transferring (exchanging) the Bell states between two pairs of resonators (bosonic qubits) interacting via a superconducting Xmon coupler can achieve fidelity as high as 96.2% (no less than 91.8%) with conservative device and circuit parameters. Because the constituents of the two registers can be reassigned *in situ* through the reconfigurable coupler-mediated pair interaction described by Eq. (4) and illustrated in Fig. 1(b), the proposed scheme can greatly reduce the complexity of the circuit and can serve as one of the fundamental building blocks for the development of more sophisticated quantum network architectures in the future. Finally, the result presented here is general and thus in principle can be applied to any type of physical qubits, such as electronic and nuclear spins, photons, atoms, and artificial atoms.

Note added. After completing this work, we noticed a work published recently by Sete *et al.* [82] on transferring a quantum state between two resonators connected by a superconducting transmission line.

ACKNOWLEDGMENTS

We thank Haohua Wang for useful discussions. S.H. acknowledges support from NSF (Grant No. PHY-1314861). S.B.Z. was supported by the Major State Basic Research Development Program of China under Grant No. 2012CB921601. Q.P.S. was supported by the National Natural Science Foundation of China under Grant No. 11247008. C.P.Y. was supported in part by the National Natural Science Foundation of China

under Grants No. 11074062 and No. 11374083, the Zhejiang Natural Science Foundation under Grant No. LZ13A040002, and the funds from Hangzhou Normal University under Grants No. HSQK0081 and No. PD13002004. This work was also supported by funds from Hangzhou City for the Hangzhou-City Quantum Information and Quantum Optics Innovation Research Team.

APPENDIX A

Suppose that qubit a_j (b_j) is coupled to the coupler C, with coupling strength g_j (μ_j) and detuning Δ_{a_j} (Δ_{b_j}). In the interaction picture, the Hamiltonian of the whole system is given by

$$H_I = \sum_{j=1}^{N}(g_j e^{i\Delta_{a_j}t}\hat{a}_j\sigma^+ + \mu_j e^{i\Delta_{b_j}t}\hat{b}_j\sigma^+ + \text{H.c.}), \quad \text{(A1)}$$

where $\Delta_{a_j} = \omega_c - \omega_{a_j}$ and $\Delta_{b_j} = \omega_c - \omega_{b_j}$.

Under the large detuning condition $\Delta_{a_j} \gg g_j$ and $\Delta_{b_j} \gg \mu_j$, and when the detunings satisfy the following condition:

$$\frac{|\Delta_{\alpha_j} - \Delta_{\beta_k}|}{\Delta_{\alpha_j}^{-1} + \Delta_{\beta_k}^{-1}} \gg g_j g_k, \mu_j\mu_k, g_j\mu_k, \; j \neq k \quad \text{(A2)}$$

(where $\alpha_j \in \{a_j, b_j\}$ and $\beta_k \in \{a_k, b_k\}$), we can obtain the effective Hamiltonian $H_{\text{eff}} = H_0 + H_{\text{int}}$, with

$$H_0 = \sum_{j=1}^{N}\left(\frac{g_j^2}{\Delta_{a_j}}\hat{a}_j\hat{a}_j^\dagger + \frac{\mu_j^2}{\Delta_{b_j}}\hat{b}_j\hat{b}_j^\dagger\right)|e\rangle\langle e| - \sum_{j=1}^{N}\left(\frac{g_j^2}{\Delta_{a_j}}\hat{a}_j^\dagger\hat{a}_j + \frac{\mu_j^2}{\Delta_{b_j}}\hat{b}_j^\dagger\hat{b}_j\right)|g\rangle\langle g|, \quad \text{(A3)}$$

$$H_{\text{int}} = \sum_{j=1}^{N}\lambda_j[e^{i(\Delta_{a_j}-\Delta_{b_j})t}\hat{a}_j\hat{b}_j^\dagger + \text{H.c.}](|e\rangle\langle e| - |g\rangle\langle g|), \quad \text{(A4)}$$

where $\lambda_j = \frac{g_j\mu_j}{2}(\Delta_{a_j}^{-1} + \Delta_{b_j}^{-1})$. When the coupler C is initially in the ground state $|g\rangle$, it will remain in this state as the Hamiltonians H_0 and H_{int} cannot induce any transition for the coupler. In this case, the Hamiltonians H_0 and H_{int} reduce to

$$H_0 = -\sum_{j=1}^{N}\left(\frac{g_j^2}{\Delta_{a_j}}\hat{a}_j^\dagger\hat{a}_j + \frac{\mu_j^2}{\Delta_{b_j}}\hat{b}_j^\dagger\hat{b}_j\right)|g\rangle\langle g|, \quad \text{(A5)}$$

$$H_{\text{int}} = -\sum_{j=1}^{N}\lambda_j[e^{i(\Delta_{a_j}-\Delta_{b_j})t}\hat{a}_j\hat{b}_j^\dagger + \text{H.c.}]|g\rangle\langle g|. \quad \text{(A6)}$$

In a new interaction picture with respect to the Hamiltonian H_0, we obtain

$$H'_{\text{int}} = e^{iH_0t}H_{\text{int}}e^{-iH_0t} = -\sum_{j=1}^{N}\lambda_j[e^{i(g_j^2/\Delta_{a_j}-\mu_j^2/\Delta_{b_j})t}e^{i(\Delta_{a_j}-\Delta_{b_j})t}\hat{a}_j\hat{b}_j^\dagger + \text{H.c.}]|g\rangle\langle g|. \quad \text{(A7)}$$

For the setting

$$g_j^2/\Delta_{a_j} - \mu_j^2/\Delta_{b_j} = -(\Delta_{a_j} - \Delta_{b_j}), \quad \text{(A8)}$$

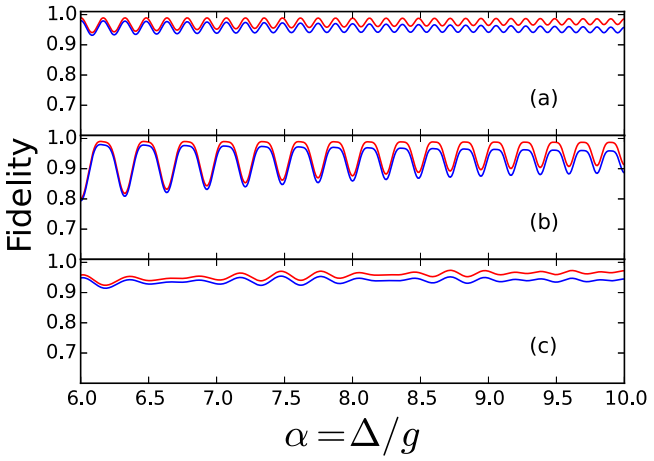

FIG. 6. (Color online) Fidelity vs α for the Bell-state transfer. Parts (a), (b), and (c) correspond to transferring the Bell states $|\psi^+\rangle$, $|\psi^-\rangle$, and $|\phi^\pm\rangle$, respectively. Here, the red curves are plotted without considering the interresonator cross-talks, while the blue ones take the weak interresonator cross-talks into account.

the Hamiltonian (17) becomes

$$H'_{\text{int}} = -\sum_{j=1}^{N}\lambda_j(\hat{a}_j\hat{b}_j^\dagger + \hat{a}_j^\dagger\hat{b}_j)|g\rangle\langle g|, \quad \text{(A9)}$$

which is exactly the one given in Eq. (5) after dropping the atomic operator $|g\rangle\langle g|$.

Note that condition (18) can be achieved by setting

$$\Delta_{b_j} = \frac{\Delta_{a_j}^2 + g_j^2 + \sqrt{(\Delta_{a_j}^2 + g_j^2)^2 - 4\Delta_{a_j}^2\mu_j^2}}{2\Delta_{a_j}}. \quad \text{(A10)}$$

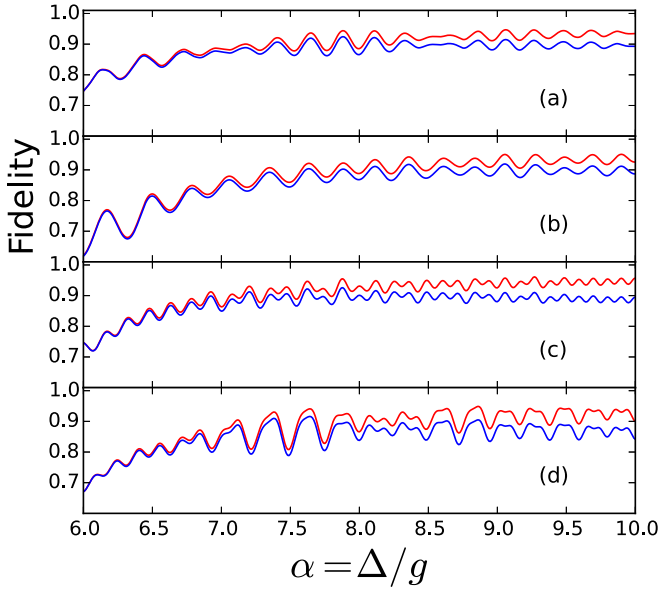

FIG. 7. (Color online) Fidelity vs α for the Bell-state exchange. Parts (a), (b), (c), and (d) correspond to exchanging the Bell states, i.e., $|\psi^+\rangle$ with $|\psi^-\rangle$, $|\phi^+\rangle$ with $|\phi^-\rangle$, $|\phi^\pm\rangle$ with $|\psi^+\rangle$, and $|\phi^\pm\rangle$ with $|\psi^-\rangle$, respectively. Here, the red curves are plotted without considering the interresonator cross-talks, while the blue ones are plotted by taking the weak interresonator cross-talks into account.

For $g_j = \mu_j$, we have $\Delta_{b_j} = \Delta_{a_j}$, i.e., the case that we discussed previously. In contrast, for $g_j \neq \mu_j$, we have $\Delta_{b_j} \neq \Delta_{a_j}$ from Eq. (20). This result implies that if the coupling g_j is not equivalent to μ_j, one can still obtain the *time-independent* effective Hamiltonian (5) or (19) by setting the detuning Δ_{b_j} slightly different from Δ_{a_j}.

APPENDIX B

When the intercavity cross-talk between resonators is considered, the Hamiltonian (1) is modified as follows:

$$\begin{aligned} H_{\rm I}' = & \sum_{j=1}^{2}(g_j e^{i\Delta_j t}\hat{a}_j\sigma^+ + \mu_j e^{i\Delta_j t}\hat{b}_j\sigma^+ + {\rm H.c.}) \\ & + \left(g_{a_1a_2}e^{i\delta t}a_1a_2^\dagger + g_{a_1b_2}e^{i\delta t}a_1b_2^\dagger + {\rm H.c.}\right) \\ & + \left(g_{a_2b_1}e^{-i\delta t}a_2b_1^\dagger + g_{b_2b_1}e^{-i\delta t}b_2b_1^\dagger + {\rm H.c.}\right) \\ & + \left(g_{a_1b_1}a_1b_1^\dagger + g_{a_2b_2}a_2b_2^\dagger + {\rm H.c.}\right), \end{aligned} \tag{B1}$$

where the terms in the last three lines represent the intercavity cross-talk between any two resonators, with the coupling constants $(g_{a_1a_2}, g_{a_1b_2}, g_{a_2b_1}, g_{b_2b_1}, g_{a_1b_1}, g_{a_2b_2})$ and detuning $\delta = \omega_{a_2} - \omega_{a_1} = \omega_{b_2} - \omega_{a_1} = \omega_{a_2} - \omega_{b_1} = \omega_{b_2} - \omega_{b_1}$ of the two associated resonators, due to $\omega_{a_1} = \omega_{b_1}$ and $\omega_{a_2} = \omega_{b_2}$.

The numerical simulation is performed by solving the master equation (10), with the Hamiltonian $H_{\rm I}$ there replaced by $H_{\rm I}'$. For simplicity, we set $g_{a_1a_2} = g_{a_1b_2} = g_{a_2b_1} = g_{b_2b_1} = g_{a_1b_1} = g_{a_2b_2} \equiv 0.01g$ (a conservative consideration for weak direct interresonator cross-talks). In our numerical simulation, the detuning setting $\Delta_1 = -\Delta_2 = \Delta$, the coupler-resonator coupling constants $g_1 = \mu_1 = g_2 = \mu_2 = g = 2\pi \times 40$ MHz, the resonator photon lifetime, and the decoherence time of the coupler are the same as those used for Figs. 4 and 5 of the main text. The operational fidelity as a function of the dimensionless detuning $\alpha \equiv \Delta/g$ in the range of $6 \leqslant \alpha \leqslant 10$ for Bell state transfer and exchange is plotted in Figs. 6 and 7, respectively. Comparing Fig. 6 (7) with Fig. 4 (5) of the main text, it can be seen that the high fidelity is hardly affected by weak direct interresonator cross-talks for both Bell state transfer and exchange.

[1] P. W. Shor, in *Proceedings of the 35th Annual Symposium on Foundations of Computer Science*, edited by S. Goldwasser (IEEE Computer Society Press, Los Alamitos, CA, 1994), Vol. 124.
[2] A. K. Ekert, Phys. Rev. Lett. **67**, 661 (1991).
[3] C. H. Bennett, G. Brassard, and N. D. Mermin, Phys. Rev. Lett. **68**, 557 (1992).
[4] J. I. Cirac and P. Zoller, Phys. Rev. Lett. **74**, 4091 (1995).
[5] D. Loss and D. P. DiVincenzo, Phys. Rev. A **57**, 120 (1998).
[6] C. H. Bennett, Phys. Rev. Lett. **68**, 3121 (1992).
[7] C. H. Bennett, G. Brassard, C. Crepéau, R. Jozsa, A. Peres, and W. K. Wootters, Phys. Rev. Lett. **70**, 1895 (1993).
[8] M. H. Y. Moussa, Phys. Rev. A **55**, R3287 (1997).
[9] M. A. Nielsen and C. M. Caves, Phys. Rev. A **55**, 2547 (1997).
[10] V. Bužek and M. Hillery, Phys. Rev. A **54**, 1844 (1996).
[11] V. Bužek, S. L. Braunstein, M. Hillery, and D. Bruß, Phys. Rev. A **56**, 3446 (1997).
[12] T. Yu and J. H. Eberly, Science **323**, 598 (2009).
[13] Y. F. Huang, B. H. Liu, L. Peng, Y. H. Li, L. Li, C. F. Li, and G. C. Guo, Nat. Commun. **2**, 546 (2011).
[14] X. C. Yao, T. X. Wang, P. Xu, H. Lu, G. S. Pan, X. H. Bao, C. Z. Peng, C. Y. Lu, Y. A. Chen, and J. W. Pan, Nat. Photon. **6**, 225 (2012).
[15] T. Monz, P. Schindler, J. T. Barreiro, M. Chwalla, D. Nigg, W. A. Coish, M. Harlander, W. Hänsel, M. Hennrich, and R. Blatt, Phys. Rev. Lett. **106**, 130506 (2011).
[16] E. Hagley, X. Maître, G. Nogues, C. Wunderlich, M. Brune, J. M. Raimond, and S. Haroche, Phys. Rev. Lett. **79**, 1 (1997).
[17] S. Osnaghi, P. Bertet, A. Auffeves, P. Maioli, M. Brune, J. M. Raimond, and S. Haroche, Phys. Rev. Lett. **87**, 037902 (2001).
[18] G. Chen, N. H. Bonadeo, D. G. Steel, D. Gammon, D. S. Katzer, D. Park, and L. J. Sham, Science **289**, 1906 (2000).
[19] F. Dolde, V. Bergholm, Y. Wang, I. Jakobi, S. Pezzagna, J. Meijer, F. Jelezko, P. Neumann, T. Schulte-Herbrüeggen, J. Biamonte, and J. Wrachtrup, Nat. Commun. **5**, 3371 (2014).
[20] P. J. Leek, S. Filipp, P. Maurer, M. Baur, R. Bianchetti, J. M. Fink, M. Göppl, L. Steffen, and A. Wallraff, Phys. Rev. B **79**, 180511(R) (2009).
[21] L. DiCarlo, J. M. Chow, J. M. Gambetta, L. S. Bishop, B. R. Johnson, D. I. Schuster, J. Majer, A. Blais, L. Frunzio, S. M. Girvin, and R. J. Schoelkopf, Nature (London) **460**, 240 (2009).
[22] M. Ansmann, H. Wang, R. C. Bialczak, M. Hofheinz, E. Lucero, M. Neeley, A. D. O'Connell, D. Sank, M. Weides, J. Wenner, A. N. Cleland, and J. M. Martinis, Nature (London) **461**, 504 (2009).
[23] J. M. Chow, L. DiCarlo, J. M. Gambetta, A. Nunnenkamp, L. S. Bishop, L. Frunzio, M. H. Devoret, S. M. Girvin, and R. J. Schoelkopf, Phys. Rev. A **81**, 062325 (2010).
[24] L. DiCarlo, M. D. Reed, L. Sun, B. R. Johnson, J. M. Chow, J. M. Gambetta, L. Frunzio, S. M. Girvin, M. H. Devoret, and R. J. Schoelkopf, Nature (London) **467**, 574 (2010).
[25] R. Barends, J. Kelly, A. Megrant, A. Veitia, D. Sank, E. Jeffrey, T. C. White, J. Mutus, A. G. Fowler, B. Campbell, Y. Chen, Z. Chen, B. Chiaro, A. Dunsworth, C. Neill, P. O'Malley, P. Roushan, A. Vainsencher, J. Wenner, A. N. Korotkov, A. N. Cleland, and J. M. Martinis, Nature (London) **508**, 500 (2014).
[26] E. F. Galvão and L. Hardy, Phys. Rev. A **62**, 012309 (2000).
[27] T. J. Johnson, S. D. Bartlett, and B. C. Sanders, Phys. Rev. A **66**, 042326 (2002).
[28] W. P. Bowen, N. Treps, B. C. Buchler, R. Schnabel, T. C. Ralph, H.-A. Bachor, T. Symul, and P. K. Lam, Phys. Rev. A **67**, 032302 (2003).
[29] G. Gordon and G. Rigolin, Phys. Rev. A **73**, 042309 (2006).
[30] B. G. Taketani, F. de Melo, and R. L. de Matos Filho, Phys. Rev. A **85**, 020301(R) (2012).
[31] D. Bouwmeester, J. W. Pan, K. Mattle, M. Eibl, H. Weinfurter, and A. Zeilinger, Nature (London) **390**, 575 (1997).
[32] A. Furusawa, J. L. Sørensen, S. L. Braunstein, C. A. Fuchs, H. J. Kimble, and E. S. Polzik, Science **282**, 706 (1998).

[33] N. Lee, H. Benichi, Y. Takeno, S. Takeda, J. Webb, E. Huntington, and A. Furusawa, Science **332**, 330 (2011).
[34] X. M. Jin, J. G. Ren, B. Yang, Z. H. Yi, F. Zhou, X. F. Xu, S. K. Wang, D. Yang, Y. F. Hu, S. Jiang, T. Yang, H. Yin, K. Chen, C. Z. Peng, and J. W. Pan, Nat. Photon. **4**, 376 (2010).
[35] J. Yin, J. G. Ren, H. Lu, Y. Cao, H. L. Yong, Y. P. Wu, C. Liu, S. K. Liao, F. Zhou, Y. Jiang, X. D. Cai, P. Xu, G. S. Pan, J. J. Jia, Y. M. Huang, H. Yin, J. Y. Wang, Y. A. Chen, C. Z. Peng, and J. W. Pan, Nature (London) **488**, 185 (2012).
[36] M. Baur, A. Fedorov, L. Steffen, S. Filipp, M. P. da Silva, and A. Wallraff, Phys. Rev. Lett. **108**, 040502 (2012).
[37] L. Steffen, Y. Salathe, M. Oppliger, P. Kurpiers, M. Baur, C. Lang, C. Eichler, G. Puebla-Hellmann, A. Fedorov, and A. Wallraff, Nature (London) **500**, 319 (2013).
[38] J. Majer, J. M. Chow, J. M. Gambetta, J. Koch, B. R. Johnson, J. A. Schreier, L. Frunzio, D. I. Schuster, A. A. Houck, A. Wallraff, A. Blais, M. H. Devoret, S. M. Girvin, and R. J. Schoelkopf, Nature (London) **449**, 443 (2007).
[39] M. A. Sillanpää, J. I. Park, and R. W. Simmonds, Nature (London) **449**, 438 (2007).
[40] J. I. Cirac, P. Zoller, H. J. Kimble, and H. Mabuchi, Phys. Rev. Lett. **78**, 3221 (1997).
[41] T. Pellizzari, Phys. Rev. Lett. **79**, 5242 (1997).
[42] A. Serafini, S. Mancini, and S. Bose, Phys. Rev. Lett. **96**, 010503 (2006).
[43] S. Ritter, C. Nölleke, C. Hahn, A. Reiserer, A. Neuzner, M. Uphoff, M. Mücke, E. Figueroa, J. Bochmann, and G. Rempe, Nature (London) **484**, 195 (2012).
[44] J. Kelly, R. Barends, A. G. Fowler, A. Megrant, E. Jeffrey, T. C. White, D. Sank, J. Y. Mutus, B. Campbell, Y. Chen, Z. Chen, B. Chiaro, A. Dunsworth, I.-C. Hoi, C. Neill, P. J. J. O'Malley, C. Quintana, P. Roushan, A. Vainsencher, J. Wenner, A. N. Cleland, and J. M. Martinis, Nature (London) **519**, 66 (2015).
[45] S. B. Zheng and G. C. Guo, Phys. Rev. Lett. **85**, 2392 (2000).
[46] M. Mariantoni, F. Deppe, A. Marx, R. Gross, F. K. Wilhelm, and E. Solano, Phys. Rev. B **78**, 104508 (2008).
[47] G. M. Reuther, D. Zueco, F. Deppe, E. Hoffmann, E. P. Menzel, T. Weißl, M. Mariantoni, S. Kohler, A. Marx, E. Solano, R. Gross, and P. Hänggi, Phys. Rev. B **81**, 144510 (2010).
[48] H. Wang, M. Mariantoni, R. C. Bialczak, M. Lenander, E. Lucero, M. Neeley, A. D. O'Connell, D. Sank, M. Weides, J. Wenner, T. Yamamoto, Y. Yin, J. Zhao, J. M. Martinis, and A. N. Cleland, Phys. Rev. Lett. **106**, 060401 (2011).
[49] J. M. Chow, J. M. Gambetta, E. Magesan, D. W. Abraham, A. W. Cross, B. R. Johnson, N. A. Masluk, C. A. Ryan, J. A. Smolin, S. J. Srinivasan, and M. Steffen, Nat. Commun. **5**, 4015 (2014).
[50] M. Mariantoni, H. Wang, R. C. Bialczak, M. Lenander, E. Lucero, M. Neeley, A. D. O'Connell, D. Sank, M. Weides, J. Wenner, T. Yamamoto, Y. Yin, J. Zhao, J. M. Martinis, and A. N. Cleland, Nat. Phys. **7**, 287 (2011).
[51] A. O. Niskanen, K. Harrabi, F. Yoshihara, Y. Nakamura, S. Lloyd, and J. S. Tsai, Science **316**, 723 (2007).
[52] M. S. Allman, F. Altomare, J. D. Whittaker, K. Cicak, D. Li, A. Sirois, J. Strong, J. D. Teufel, and R. W. Simmonds, Phys. Rev. Lett. **104**, 177004 (2010).
[53] R. C. Bialczak, M. Ansmann, M. Hofheinz, M. Lenander, E. Lucero, M. Neeley, A. D. O'Connell, D. Sank, H. Wang, M. Weides, J. Wenner, T. Yamamoto, A. N. Cleland, and J. M. Martinis, Phys. Rev. Lett. **106**, 060501 (2011).
[54] J. M. Gambetta, A. A. Houck, and A. Blais, Phys. Rev. Lett. **106**, 030502 (2011).
[55] M. Hofheinz, H. Wang, M. Ansmann, R. C. Bialczak, E. Lucero, M. Neeley, A. D. O'Connell, D. Sank, J. Wenner, J. M. Martinis, and A. N. Cleland, Nature (London) **459**, 546 (2009).
[56] J. Clarke and F. K. Wilhelm, Nature (London) **453**, 1031 (2008).
[57] M. Neeley, M. Ansmann, R. C. Bialczak, M. Hofheinz, N. Katz, E. Lucero, A. O'Connell, H. Wang, A. N. Cleland, and J. M. Martinis, Nat. Phys. **4**, 523 (2008).
[58] G. Sun, X. Wen, B. Mao, J. Chen, Y. Yu, P. Wu, and Siyuan Han, Nat. Commun. **1**, 51 (2010).
[59] J. D. Strand, M. Ware, F. Beaudoin, T. A. Ohki, B. R. Johnson, A. Blais, and B. L. T. Plourde, Phys. Rev. B **87**, 220505(R) (2013).
[60] M. Sandberg, C. M. Wilson, F. Persson, T. Bauch, G. Johansson, V. Shumeiko, T. Duty, and P. Delsing, Appl. Phys. Lett. **92**, 203501 (2008).
[61] Z. L. Wang, Y. P. Zhong, L. J. He, H. Wang, J. M. Martinis, A. N. Cleland, and Q. W. Xie, Appl. Phys. Lett. **102**, 163503 (2013).
[62] W. Chen, D. A. Bennett, V. Patel, and J. E. Lukens, Supercond. Sci. Technol. **21**, 075013 (2008).
[63] P. J. Leek, M. Baur, J. M. Fink, R. Bianchetti, L. Steffen, S. Filipp, and A. Wallraff, Phys. Rev. Lett. **104**, 100504 (2010).
[64] A. Megrant, C. Neill, R. Barends, B. Chiaro, Y. Chen, L. Feigl, J. Kelly, E. Lucero, M. Mariantoni, P. J. J. O'Malley, D. Sank, A. Vainsencher, J. Wenner, T. C. White, Y. Yin, J. Zhao, C. J. Palmstrøm, J. M. Martinis, and A. N. Cleland, Appl. Phys. Lett. **100**, 113510 (2012).
[65] A. Blais, R. S. Huang, A. Wallraff, S. M. Girvin, and R. J. Schoelkopf, Phys. Rev. A **69**, 062320 (2004).
[66] J. Q. You and F. Nori, Nature (London) **474**, 589 (2011).
[67] Z. L. Xiang, S. Ashhab, J. Q. You, and F. Nori, Rev. Mod. Phys. **85**, 623 (2013).
[68] C. P. Yang, S-I. Chu, and S. Han, Phys. Rev. A **67**, 042311 (2003).
[69] D. I. Schuster, A. A. Houck, J. A. Schreier, A. Wallraff, J. M. Gambetta, A. Blais, L. Frunzio, J. Majer, B. Johnson, M. H. Devoret, S. M. Girvin, and R. J. Schoelkopf, Nature (London) **445**, 515 (2007).
[70] F. W. Strauch, Phys. Rev. A **84**, 052313 (2011).
[71] C. W. Wu, M. Gao, H. Y. Li, Z. J. Deng, H. Y. Dai, P. X. Chen, and C. Z. Li, Phys. Rev. A **85**, 042301 (2012).
[72] M. Hua, M. J. Tao, and F. G. Deng, Phys. Rev. A **90**, 012328 (2014).
[73] E. Lucero, R. Barends, Y. Chen, J. Kelly, M. Mariantoni, A. Megrant, P. O'Malley, D. Sank, A. Vainsencher, J. Wenner, T. White, Y. Yin, A. N. Cleland, and J. M. Martinis, Nat. Phys. **8**, 719 (2012).
[74] M. Pierre, I. M. Svensson, S. R. Sathyamoorthy, G. Johansson, and P. Delsing, Appl. Phys. Lett. **104**, 232604 (2014).
[75] M. Mariantoni, H. Wang, T. Yamamoto, M. Neeley, R. C. Bialczak, Y. Chen, M. Lenander, E. Lucero, A. D. O'Connell, D. Sank, M. Weide, J. Wenner, Y. Yin, J. Zhao, A. N. Korotkov, A. N. Cleland, and J. M. Martinis, Science **334**, 61 (2011).
[76] R. Barends, J. Kelly, A. Megrant, D. Sank, E. Jeffrey, Y. Chen, Y. Yin, B. Chiaro, J. Mutus, C. Neill, P. O'Malley, P. Roushan, J. Wenner, T. C. White, A. N. Cleland, and J. M. Martinis, Phys. Rev. Lett. **111**, 080502 (2013).

[77] J. B. Chang, M. R. Vissers, A. D. Córcoles, M. Sandberg, J. Gao, D. W. Abraham, J. M. Chow, J. M. Gambetta, M. B. Rothwell, G. A. Keefe, M. Steffen, and D. P. Pappas, Appl. Phys. Lett. **103**, 012602 (2013).

[78] H. Paik, D. I. Schuster, L. S. Bishop, G. Kirchmair, G. Catelani, A. P. Sears, B. R. Johnson, M. J. Reagor, L. Frunzio, L. I. Glazman, S. M. Girvin, M. H. Devoret, and R. J. Schoelkopf, Phys. Rev. Lett. **107**, 240501 (2011).

[79] Y. Chen, C. Neill, P. Roushan, N. Leung, M. Fang, R. Barends, J. Kelly, B. Campbell, Z. Chen, B. Chiaro, A. Dunsworth, E. Jeffrey, A. Megrant, J. Y. Mutus, P. J. J. O'Malley, C. M. Quintana, D. Sank, A. Vainsencher, J. Wenner, T. C. White, M. R. Geller, A. N. Cleland, and J. M. Martinis, Phys. Rev. Lett. **113**, 220502 (2014).

[80] A. Fedorov, L. Steffen, M. Baur, M. P. da Silva, and A. Wallraff, Nature (London) **481**, 170 (2012).

[81] M. A. Nielsen and I. L. Chuang, *Quantum Computation and Quantum Information* (Cambridge University Press, Cambridge, England, 2001).

[82] E. A. Sete, E. Mlinar, and A. N. Korotkov, Phys. Rev. B **91**, 144509 (2015).